Available online at www.sciencedirect.com
ScienceDirect
C. R. Physique 7 (2006) 1101–1120
COMPTES RENDUS PHYSIQUE
http://france.elsevier.com/direct/COMREN/

Nucleation/Nucléation

Critical velocities in superfluids and the nucleation of vortices

Éric Varoquaux [a,b]

[a] *CNRS-Université Paris-sud, Laboratoire de physique des solides, bâtiment 510, 91405 Orsay cedex, France*
[b] *Commissariat à l'énergie atomique, service de physique de l'état condensé, bâtiment 772, centre de Saclay, 91191 Gif-sur-Yvette cedex, France*

Available online 28 November 2006

Abstract

The problem of critical velocities in superfluids, that is the comprehension of superfluidity breakdown by flow, has been long standing. One difficulty stems from the existence of several breakdown mechanisms. A major advance has come from the observation of single 2π phase slips, which arise from the nucleation of quantised vortices, that is, their creation ex nihilo. The statistical properties of the nucleation process in both the thermal regime and the quantum regime are identified and analysed: vortex nucleation provides a well-documented case of macroscopic quantum tunnelling (MQT). In particular, a close scrutiny of the experimental data obtained on ultra-pure ^{4}He reveals the influence of damping on tunnelling, a rare occurrence where the effect of the environment on MQT can be studied. ***To cite this article: É. Varoquaux, C. R. Physique 7 (2006).***

Résumé

Vitesses critiques dans les superfluides et nucléation de tourbillons. La vitesse critique dans les superfluides, c'est-à-dire la destruction de la superfluidité par l'écoulement du fluide, pose un problème qui perdure. Une des difficultés réside dans l'existence de plusieurs mécanismes pour cette destruction. L'observation de sauts de phase individuels de 2π, qui proviennent de la nucléation de tourbillons quantifiés, a constitué une avancée importante. L'identification et l'analyse des propriétés stochastiques du processus de nucléation, tant dans le régime classique que quantique, ont conduit à l'étude très circonstanciée d'un cas spécifique d'effet tunnel macroscopique. En particulier, l'examen fouillé des données expérimentales obtenues avec l'hélium ultra-pur a révélé l'influence de la dissipation sur l'effet tunnel, donnant par là un exemple rare d'interaction d'un processus tunnel avec son environnement macroscopique. ***Pour citer cet article : É. Varoquaux, C. R. Physique 7 (2006).***

The critical velocity in a superfluid is the threshold above which the flow of the superfluid component becomes dissipative, that is, the property of superfluidity is lost. This rather broad definition encompasses a number of different physical situations. The following overview starts with a brief description of the different brands of velocities that comply with this definition. It then joins the main trend of this Dossier by focusing on that which involves a nucleation phenomenon, namely, the nucleation of superfluid vortices.

Neither the problem of critical velocities in superfluids nor that of the nucleation of vortices is new. The former is as old as the discovery of superfluidity (see the monograph by Wilks [1]). The latter, first discussed by Vinen in the early sixties [2], has met a more tortuous fate. It was first thought, still is in some quarters, to be impossible [2] on the

E-mail address: eric.varoquaux@gmail.com (É. Varoquaux).

1631-0705/$ – see front matter
doi:10.1016/j.crhy.2006.10.023

grounds that such an extended hydrodynamical object as a vortex with a finite (quantised) circulation, involving the motion of a large number of helium atoms, would have a vanishingly small probability of occurring spontaneously. For classical ideal fluids, this is the essence of the Kelvin–Helmholtz theorem, which states that vorticity is conserved for isentropic motion of inviscid fluids. More recent experiments, probing superflow on a finer scale of length [3–5], have shown otherwise.

I give below a short account of these problems, which is hardly more than a guided tour of the four references [6–9] written by the author and his colleagues over the course of many years. More extended discussions can be found in these articles as well as more complete bibliographies. Also, a more comprehensive review is in preparation.

1. Critical velocities in superfluids

1.1. The Landau criterion

Landau [1] explained the superfluidity of helium-4 by the sharpness of the dispersion curve for elementary excitations, phonons and rotons, shown in Fig. 1, which is a property associated with the existence of a Bose–Einstein condensate. Elementary excitation energy levels $\varepsilon(p)$ being well-defined, that is, having a negligible spread in energy, very low-lying states, energy-wise and momentum-wise, are extremely scarce. An impurity, or a solid obstacle, can only exchange an energy $\varepsilon(p)$ at momentum p that exactly matches the energy of an elementary excitation of the fluid. Unless this condition can be precisely met, there is no dissipative interaction between the fluid and its surroundings: the flow is viscousless at small flow velocities.

If the superfluid moves at velocity $\mathbf{v}_\mathrm{s}$, the energy of elementary excitations in the frame of reference at rest becomes $\varepsilon + \mathbf{v}_\mathrm{s} \cdot \mathbf{p}$ [1,10]. The same holds for a moving obstacle, by Galilean invariance. If this energy turns negative, elementary excitations proliferate and superfluidity is lost. The condition on the superfluid velocity for this to happen reads:

$$v_\mathrm{s} \geqslant v_\mathrm{L} = \left.\frac{\varepsilon(p)}{p}\right|_{\min} \simeq \left.\frac{\varepsilon(p)}{p}\right|_{\mathrm{roton}} \tag{1}$$

The minimum value of ε/p for helium is very close to the roton minimum, as shown in Fig. 1. In ^{4}He at low pressure, $v_\mathrm{L} \simeq 60$ m/s. The Landau critical velocity v_L is smaller than the sound velocity $c = 220$ m/s but larger than most critical velocities measured in various experiments. For the much less dense Bose–Einstein condensed gases, which do not exhibit roton-like features, the minimum is the sound velocity, $c = \varepsilon(p)/p|_{p=0}$.

1.2. Feynman's approach

Feynman [1], following Onsager, realised that, not only would vorticity be quantised in ^{4}He in units of the quantum of circulation $\kappa_4 = 2\pi\hbar/m_4 \simeq 10^{-3}$ cm^2/s, m_4 being the mass of the helium-4 atom (which is also a property associated with the existence of a Bose–Einstein condensate), but that these vortices would be responsible for the onset of dissipation and for a critical velocity in the superfluid. The basic reason for this, as spelled out clearly by

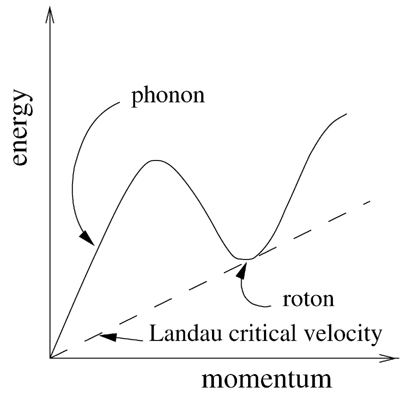

Fig. 1. Dispersion curve of the elementary excitations in superfluid ^{4}He.

Anderson [11], is that vortices can exchange energy with the potential superflow and carry this energy away, thus causing an energy loss to the superflow.

In order to evaluate a characteristic velocity associated with this process, let us consider a vortex ring of radius R. Its energy E_R and impulse P_R are expressed by [12–14]

$$E_R = \frac{1}{2}\rho_s\kappa_4^2 R\left(\ln\frac{R}{a_0} - \frac{7}{4}\right) + \mathcal{O}\left(\frac{a_0}{R}\right) \tag{2}$$

$$P_R = \pi\rho_s\kappa_4 R^2 \tag{3}$$

where a_0 is the vortex core radius, taken here as the superfluid coherence length.

Let us treat such a vortex as an elementary excitation of the superfluid, which it rightfully is, and apply Landau's criterion. The limiting velocity is reached for a radius R such that E_R/P_R is at a minimum, which occurs when R is as large as feasible, that is of the order of the channel size d. This minimum value sets the velocity at which vortices can start to appear and defines the Feynman critical velocity:

$$v_F \simeq \frac{\kappa_4}{2\pi d}\ln\left(\frac{d}{a_0}\right) \tag{4}$$

As discussed below, v_F is much closer to experimental values than the Landau critical velocity for rotons. Although this agreement is heartening, it also raises fresh questions: how do these vortices come about?

1.3. The phase slips

The phase slippage experiments that were carried out starting from the mid-eighties [5,15] confirmed Feynman and Anderson's views on dissipation in superflows [11] and brought a large measure of clarification in the critical velocity problem [6] and in the formation of vortices in superfluid ^{4}He [7]. These experimental results and their interpretation have since been largely confirmed [16–18].

Phase slips can be studied with the help of a miniature hydro-mechanical device, which is basically a flexible-diaphragm Helmholtz resonator as represented schematically in Fig. 2. This resonator is immersed in the superfluid bath. The flexible diaphragm is constituted by a Kapton membrane coated with aluminium. In the version shown in Fig. 2, there are two openings connecting the resonator chamber to the superfluid bath. One is a micro-aperture in which the critical velocity phenomenon takes place. The critical event consists in a sudden jump in the resonance amplitude which corresponds to an abrupt change in the flow velocity through the micro-aperture and a loss of resonator energy. These dissipation events are interpreted as resulting from single vortex emission, to which is associated a slip by 2π of the quantum phase difference across the micro-aperture, $\delta\varphi$, caused by the motion of the vortex across the flow stream.

The other opening is a relatively open duct and provides a parallel path to the superfluid along which the quantum phase remains well determined even when the phase slips in the micro-aperture. A quantum of circulation builds up for each 2π slip along the superfluid closed loop threading the two openings. The operation of these resonators is described in detail in the literature (see, for instance [5,19–22]).

The resonator is driven on resonance by an electrostatic *ac*-drive applied to the aluminium-coated flexible membrane at a constant level. In the absence of dissipation, the resonance motion increases linearly in amplitude under

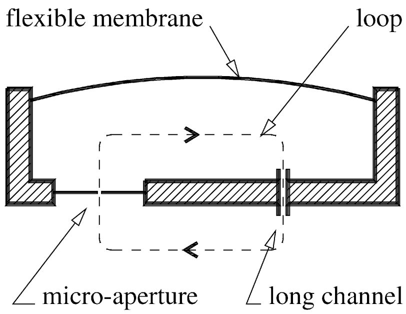

Fig. 2. Schematic drawing of the flexible-diaphragm Helmholtz resonator.

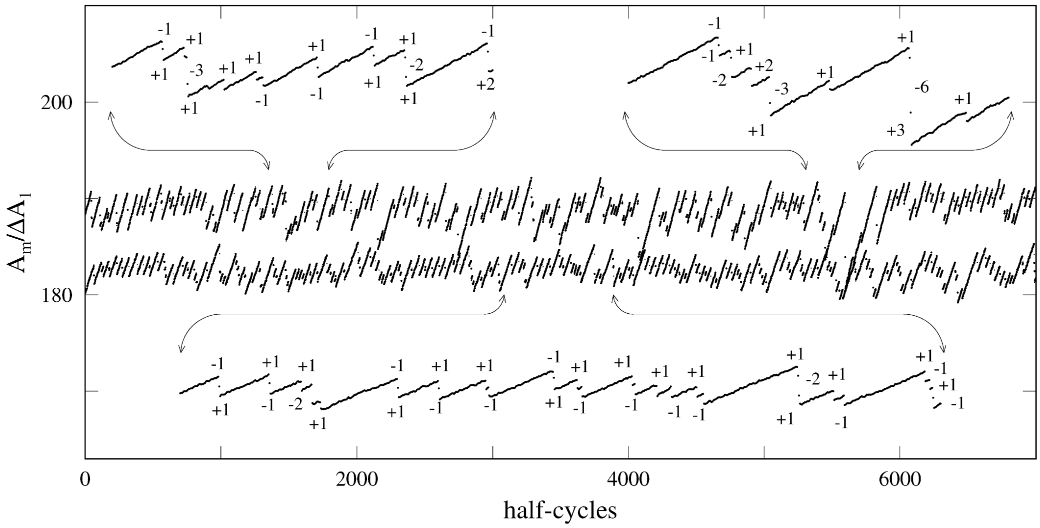

Fig. 3. Peak amplitude charts at 100.7 mK (top) and 201.5 mK (bottom) at saturated vapour pressure in ultra-pure ^{4}He with a ^{3}He impurity concentration less than 10^{-9}. Peak absolute amplitudes during each half-cycle of the resonator motion at 12.5 Hz are plotted as a function of half-cycle index; time runs from left to right. The peak membrane amplitude A_m is normalised to the amplitude jump of a single slip ΔA_1. The traces at the very top and bottom of the graph, expanded from the main traces as indicated by curly arrows, show the slip sizes in signed winding numbers of the quantum phase (according to flow direction, in and out of the resonator chamber).

the action of the drive. The displacement of the membrane, which is proportional to the total flow in and out of the resonator, is monitored by an electrodynamic displacement sensor with a SQUID amplifier,[1] the output of which is converted into a digital signal by a fast analogue-to-digital converter. The peak amplitudes of the membrane motion A_m for each successive positive-going and negative-going half-cycle of the resonance are measured and stored digitally in real time. The raw data consist of peak amplitude charts as represented in Fig. 3. Phase slips are seen as sudden drops of the peak amplitude from one half-cycle to the next.

The pattern of these peak amplitude data is processed numerically to identify all the slips and their multiplicity, and to obtain the state of quantised circulation trapped in the resonator loop, labelled j. The actual flow in the micro-aperture is the sum of the flow driven by the membrane and of the persistent flow threading the micro-aperture and the parallel channel, which depends on the quantum state of the loop j. The amplitude drop ΔA_1 caused by a single phase slip in a given half-cycle of the resonance corresponds to a change of $\delta\varphi$ by exactly 2π. Normalising the membrane displacement A_m by ΔA_1 as done in Fig. 3 provides a self-calibration of the data that is independent of less well known quantities such as the membrane stiffness, and the calibration factor of the displacement sensor.

In the following, aperture velocities are expressed by the number of turns $\delta\varphi/2\pi$ by which the quantum-mechanical phase winds across the aperture.[2] The actual flow velocity averaged over the cross-section of the micro-aperture is proportional to $\delta\varphi$, the multiplying factor being $\hbar/m_4 l_\mathrm{h}$. The hydraulic length l_h of the micro-aperture is of the order of 1 µm in the experiments shown in Fig. 3.

1.4. Phase-slippage experimental results

The observation of phase slips in ^{4}He has led to a number of quite significant results that have shed light onto the previously indecipherable critical velocity problem. I summarise below the most important qualitative features and their implications:

---

[1] SQUID is an acronym for Superconducting QUantum Interferometric Device. The present sensitivity of the displacement sensor is $\sim 10^{-15}$ m.

[2] Phase winding numbers are related to velocities in cm/s by multiplication by l_h/κ_4, the "hydraulic" length l_h characterising the geometry of the aperture. For a phase slip by 2π, the phase winding number changes by one unit and the trapped circulation in the resonator loop by one quantum.

1. The critical velocity threshold, which can be seen on time charts such as that shown in Fig. 3, is markedly temperature-dependent down to below 200 mK and reaches a well-defined plateau below 150 mK. These features can been seen in Fig. 5 and will be discussed below. As the thermodynamic properties of superfluid ^{4}He are very nearly independent of temperature below 1 K, this observation indicates that the critical process in action is not governed solely by hydrodynamics. It can be suspected that statistical mechanics plays a leading role.
2. Aperture-size is not found to be a relevant factor. This feature and the temperature dependence mentioned above are in sharp contrast with the Feynman critical velocity, which, according to Eq. (4), exhibits a well-characterised dependence on size and none on temperature.
3. The actual velocity threshold for phase slips shows significant scatter from one slip to the next in a given sequence, as can be seen in Fig. 3. This scatter lies much above the background noise level of detection of the peak amplitudes of the resonator motion. It represents a genuine stochastic property of the process at work, which turns out to display a temperature dependence similar to that of the critical velocity shown in Fig. 6.
4. The phase slip pattern shows quite reproducible properties in the course of a given cool-down as long as the experimental cell is kept at a temperature below 10–15 K. If the temperature is cycled up to nitrogen temperature or above, small changes to the critical threshold and the pattern itself can occur. This is likely due to changes in the surface state of the cell, i.e. contamination of the micro-aperture walls by solidified gases.
5. Quite importantly, phase slips are the signature that *quantised vortices* are created in aperture flow above a well-defined threshold of flow velocity. This statement arises from the highly reproducible phase change, which is measured to be very nearly 2π and to amount to changes of precisely one quantum of circulation in the superfluid loop threading the micro-aperture and the long parallel channel (see Fig. 2). A detailed scenario for the occurrence and development of phase slips that shows how the phase difference by 2π develops has been described by Burkhart et al. [23] and is discussed below. Different mechanisms have been proposed [24–26] for which it is unclear that the end product of the nucleation process is actually a vortex.

Critical velocities and phase slips in the superfluid phases of ^{3}He show different features that will be briefly touched upon in Section 5.

1.5. Several kinds of critical velocities

The compilation of the critical velocity data in various apertures and channels from various sources available in the literature presented at the Exeter Meeting in 1990 [6] and shown in Fig. 4 has not been updated. Two different critical velocity regimes appear clearly on the graph in Fig. 4, a fast regime for small apertures, of the phase-slip type, and a slower regime for larger channels, of the Feynman type. More recent data confirm this behaviour. In some occasions, switching between these two types of critical velocity has been observed in the course of the same cool-down [27,28].

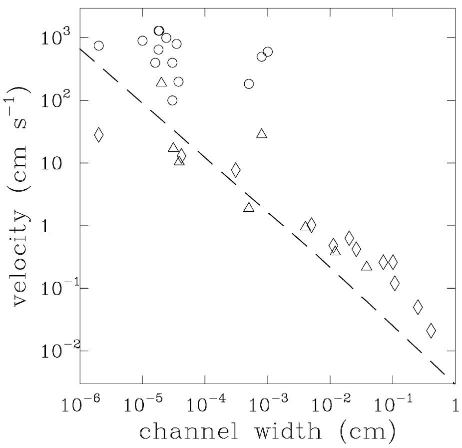

Fig. 4. Critical velocity data vs channel width ◇—older data [1]; ○ and △—temperature-dependent and temperature-independent data, from Ref. [6]. For the temperature-dependent data, the highest value, i.e. that at the lowest temperature, has been retained. The dash–dash line is obtained from the Feynman criterion, Eq. (4).

The data points from various sources [6] for these two different types of critical velocity do not fall on well-defined lines as can be seen in Fig. 4 but merely bunch into clusters of points. As already stated, critical velocity values in apertures and capillaries are not very reproducible from experiment to experiment, indicating that some less-well-controlled parameters, besides size, temperature and pressure, also exert an influence.

As a basis for comparison, it is worthwhile to also mention the findings of the ion propagation studies in superfluid ^{4}He at various pressures, which have been reviewed by McClintock and Bowley [29,30]. Ions can be created in liquid helium and accelerated by an electric field until they reach a critical velocity. The resulting drift velocities are measured by time-of-flight techniques. For negative ions, hollow bubbles 30 Å in diameter with an electron inside, two different behaviours are observed:

- Below about 10 bars, vortex rings are created, on the core of which the electron gets trapped: the drift velocity suddenly drops from that of the negatively charged bubble to the much slower vortex velocity [31].
- Above 10 bars, the accelerated ion runs into the roton creation barrier before vortex rings can be created. The Landau critical velocity is observed to decrease from about 60 m/s at SVP down to 46 m/s at 24 bars as the roton parameters change with pressure while the vortex creation velocity increases with pressure.
- Around 10 bars, both critical velocities, the Landau critical velocity for the formation of rotons and that for the formation of vortex rings can be observed to occur simultaneously because ions can be accelerated above the threshold for roton emission.

These ion propagation measurements provide a vivid illustration not only of the existence of a critical velocity obeying the Landau criterion but also that roton creation and vortex formation constitute different phenomena and can exist concurrently.[3] The vortex emission threshold displays other noteworthy features. It depends on temperature in a non-trivial way, comparable to that of the phase-slip critical velocity with the appearance of a plateau below $\sim$300 mK. It also shows the marked dependence on ^{3}He impurity concentration observed for phase slips in micro-aperture flows but not in larger channels. In both ion propagation and aperture flow measurements, vortex formation displays very similar features.

Altogether, a careful study of the experimental data in superfluid ^{4}He reveals three different, well-defined, types of critical velocities, one which is the celebrated Landau critical velocity, another which seems related to the Feynman criterion with all the uncertainties on the hydrodynamical process of vortex creation in larger channels, and a third, for phase slips, which is in want of an explanation: how are the vortices of phase slips in aperture flow created, and how does the situation differ from that in larger channels?

The short answer, based on qualitative evidence, is that the temperature dependence of v_c and its stochastic properties clearly point toward a process of nucleation by thermal activation above $\sim$150 mK or so and by quantum tunnelling below. This conclusion contradicts our daily observations of the formation of whirlpools and eddies. It will be seen to hold in ^{4}He because the nucleated vortices have nanometric size, a fact that came to be appreciated because of the detailed analysis of phase slippage observations that I briefly relate below.

2. Phase slip critical velocity

A more firmly established answer to the questions formulated above comes from a quantitative analysis of the experimental data for phase slips. These experiments do provide clues that, pieced together, conclusively show that, in small apertures, vortices are indeed nucleated by thermal activation above about 150 mK, and by quantum tunnelling below.

Let me begin with some preliminary remarks. A glance at Fig. 3 reveals that the critical velocity threshold itself needs to be defined. Also, the local value of the critical velocity is not measured directly. Experiments record the mean value of the volume flow, which is assumed to be proportional to the local values of the flow field velocity; this assumption breaks down in the presence of vorticity and has to be taken with a grain of salt (see Section 5). The value of the critical threshold is not even reproducible from one cool-down to the next with the same experimental cell. This

[3] A noteworthy attempt to by-pass this experimental finding is that of Ref. [26].

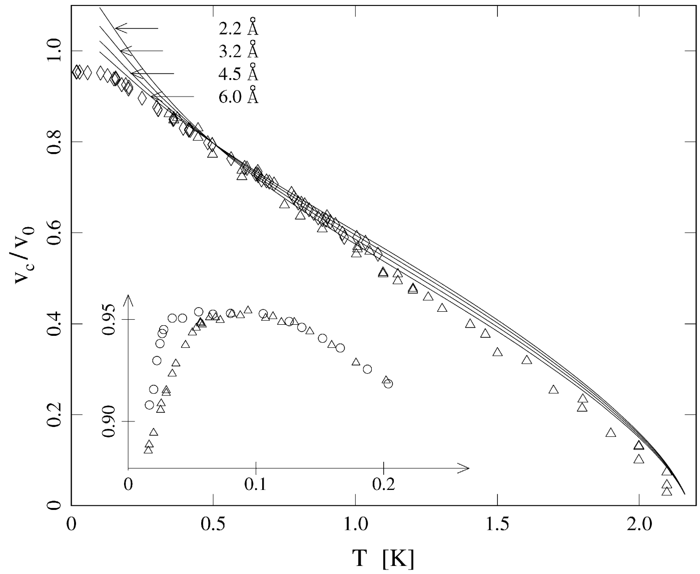

Fig. 5. Critical velocity, normalised to the zero temperature *linear* extrapolation value v_0, vs T, in kelvin: (◇), Ref. [7], for ultra-pure ^{4}He; (△), Ref. [32]. The plain curves are computed from the half-ring model (see Section 4) for $a_0 = 2.2$, 3.2, 4.5, 6.0 Å and are normalised to match the experimental value at 0.5 K. The inset shows the influence of ^{3}He impurities on v_c: (○), 3 ppb ^{3}He in ^{4}He; (△), 45 ppb, from Ref. [33].

lack of reproducibility in the measurements, both in micro-apertures and in larger channels, has obscured the critical velocity problem for a long time. It must, however, be considered as an integral part of the problem.

Now, on with the real topic of this Dossier: nucleation. The first piece of evidence for the nucleation of vortices, that is their creation ex nihilo, rests on the temperature dependence of the phase-slip critical velocity shown in Fig. 5, which increases in a near-linear manner when the temperature decreases from 2 to ∼0.2 K. I mean by linear a functional dependence going as $v_c = v_0(1 - T/T_0)$. As can be seen in Fig. 5, the data depart from this linear dependence below 200 mK, where they reach a plateau, and above 2 K because the critical velocity goes to zero at T_λ.

This temperature dependence, first observed in 1985 at Orsay [5] is now a well-established experimental fact [8]. It came as a surprise at first because the critical velocities observed before were temperature-independent below ∼1 K. As the quantum fluid is nearly fully in its ground state below 1 K—the normal fluid fraction becomes less than 1%—one is led to suspect, as was done in Ref. [5], that an Arrhenius-type process must come into play. If such is the case, that is, if a thermal fluctuation in the fluid with an energy of at most a few $k_B T$ can trigger the appearance of a fully-formed vortex out of nowhere, the energy of this vortex must also be of the order of a few $k_B T$: it must be a very small vortex. But very small vortices require rather large superfluid velocities to sustain themselves. A careful analysis of the situation is thus in order.

The nucleation rate for thermally activated process is given in terms of the activation energy by Arrhenius' law:

$$\Gamma_K = \frac{\omega_0}{2\pi}\left[\left(1+\alpha^2\right)^{1/2} - \alpha\right]\exp\left\{-\frac{E_a}{k_B T}\right\} \tag{5}$$

where $\omega_0/2\pi$ is the attempt frequency and E_a the activation energy. The correction for dissipation has been introduced by Kramers to describe the escape of a particle trapped in a potential well and interacting with a thermal bath in its environment. The particle undergoes Brownian motion fluctuations and experiences dissipation. This dissipation is characterised by a dimensionless coefficient $\alpha = 1/2\omega_0\tau$, τ being the time of relaxation of the system toward equilibrium. In superfluid helium, dissipation is small, although some dissipation is necessary for the system to reach equilibrium with its environment. Its influence on the thermal activation rate is very small and will be neglected in the following. However, this will not be the case anymore in the quantum regime.

Let us derive the expression for the critical velocity that stems from the Arrhenius rate, Eq. (5). In experiments performed in a Helmholtz resonator, such as those shown in Fig. 3, the velocity varies periodically at the resonance

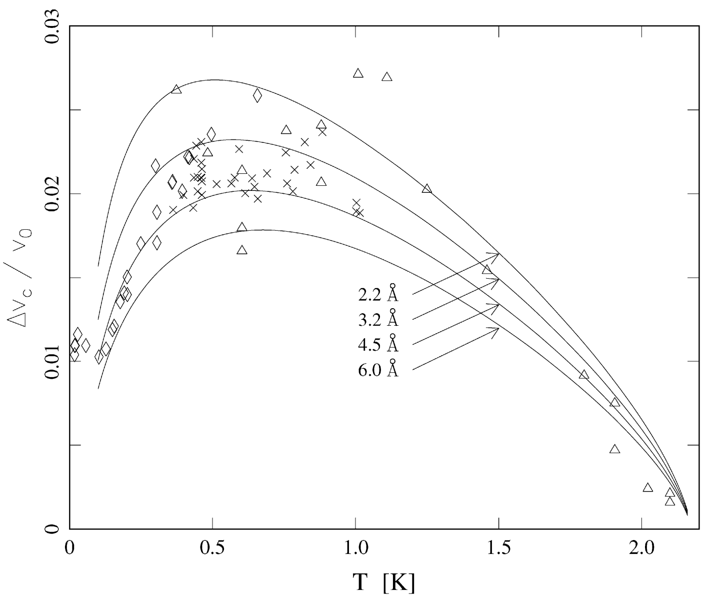

Fig. 6. Statistical width of the critical velocity transition, normalised to the linear extrapolation limit at $T = 0$, v_0, in terms of temperature: (◊), Ref. [7]; (△), Ref. [32]; (×), Ref. [34].

frequency as $v_\mathrm{p}\cos(\omega t)$, v_p being the peak velocity. The probability that a phase slip takes place during the half-cycle $\omega t_\mathrm{i} = -\pi/2$, $\omega t_\mathrm{f} = \pi/2$ is

$$p = 1 - \exp\left\{-\int_{t_\mathrm{i}}^{t_\mathrm{f}} \Gamma\big(P, T, v_\mathrm{p}\cos(\omega t')\big)\right\}\mathrm{d}t' = 1 - \exp\left\{-\frac{\omega_0}{2\pi\omega}\sqrt{\frac{-2\pi k_\mathrm{B}T}{v_\mathrm{p}\partial E_\mathrm{a}/\partial v|_{t=0}}}\exp\left\{-\frac{E_\mathrm{a}}{k_\mathrm{B}T}\right\}\right\} \tag{6}$$

Eq. (6) results from an asymptotic evaluation of the integral at the saddle point $t = 0$. The accuracy of the asymptotic evaluation (6) becomes questionable for $T \to 0$ as the energy barrier vanishes. But, as we shall see, quantum effects take over and the energy barrier never actually vanishes.

The critical velocity v_c is defined as the velocity for which $p = 1/2$. This definition is independent of the experimental setup, except for the occurrence in Eq. (6) of the natural frequency of the Helmholtz resonator ω. The implicit relation between v_c and E_a then reads:

$$\frac{\omega_0}{2\pi\omega}\sqrt{\frac{-2\pi k_\mathrm{B}T}{v_\mathrm{c}\partial E_\mathrm{a}/\partial v|_{v_\mathrm{c}}}}\exp\left\{-\frac{E_\mathrm{a}(P, T, v_\mathrm{c})}{k_\mathrm{B}T}\right\} = \ln 2 \tag{7}$$

We note that, in Eq. (7), the attempt frequency is normalised by the resonator drive frequency: the Brownian particle attempts to escape from the potential well at rate $\omega_0/2\pi$ but an escape event is likely only in the time window in a given half-cycle of the resonance during which the energy barrier stays close to its minimum value $E_\mathrm{a}(v_\mathrm{c})$. This time interval is inversely proportional to ω, which explains why an instrumental parameter gets its way into Eqs. (6) and (7).

The velocity at which individual critical events take place is a stochastic quantity. Its statistical spread can be characterised by the 'width' of the probability distribution defined [7,35] as the inverse of the slope of the distribution at v_c, $(\partial p/\partial v|_{v_\mathrm{c}})^{-1}$. This critical width is found to be expressed by:

$$\Delta v_\mathrm{c} = -\frac{2}{\ln 2}\left[\frac{1}{2}\left\{\frac{1}{v_\mathrm{c}} + \left.\frac{\partial^2 E_\mathrm{a}}{\partial v^2}\right|_{v_\mathrm{c}} \Big/ \left.\frac{\partial E_\mathrm{a}}{\partial v}\right|_{v_\mathrm{c}}\right\} + \frac{1}{k_\mathrm{B}T}\left.\frac{\partial E_\mathrm{a}}{\partial v}\right|_{v_\mathrm{c}}\right]^{-1} \tag{8}$$

In the experiments, at low temperatures and large critical velocities, the quantity in curly brackets in the right-hand side of Eq. (8) is small with respect to the last term so that the width is simply expressed as $\Delta v_\mathrm{c} = -(2/\ln 2)k_\mathrm{B}T(\partial E_\mathrm{a}/\partial v|_{v_\mathrm{c}})^{-1}$. Thus, the statistical width is an approximate measure of the inverse of the slope of E_a in terms of v.

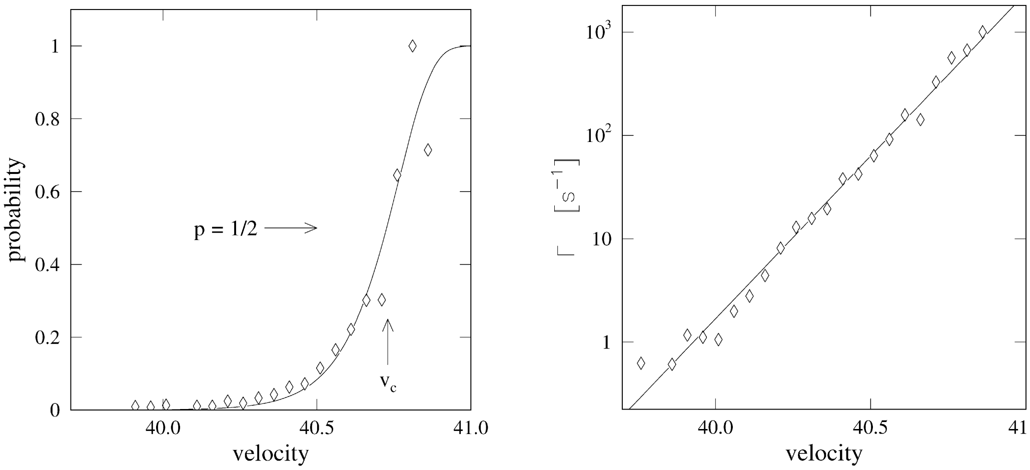

Fig. 7. Left: Probability p vs slip velocity in winding number. The plain curve is a non-linear least square fit to the analytical form (6), which contains two unknown parameters, v_c and Δv_c. The critical velocity is defined as that for which $p = 1/2$. Right: Nucleation rate Γ expressed in s^{-1} vs slip velocity in winding number in ultra-pure ^{4}He at 17.70 mK and saturated vapour pressure on a semi-logarithmic scale. The line is a linear fit to the data.

We now have precise definitions for v_c and Δv_c. These quantities are derived from p, itself obtained by integrating the histograms of the number of nucleation events ordered in velocity bins. The outcome of this procedure is illustrated in Fig. 7: p shows an asymmetric-S shape characteristic of the double exponential dependence of p on v, Eq. (6), a consequence of Arrhenius' law, Eq. (5), being plugged into a Poisson probability distribution. The observation of this asymmetric-S probability distribution constitutes another experimental clue for the existence of a nucleation process.

The quantities v_c and Δv_c are easily extracted from the probability curves $p(v)$, but going from v_c and $\Delta v_c = -(2/\ln 2)k_B T(\partial E_a/\partial v|_{v_c})^{-1}$ back to $E_a(v)$ and ω by numerical integration of the differential equation (7) requires more work and introduces additional errors. As discussed in Ref. [9], an improved procedure consists in obtaining directly the escape rate Γ from the phase slip data. This quantity is the ratio, for a given velocity bin, of the number of slips which have occurred at that velocity to the total time spent by the system at that given velocity. The outcome of this procedure is illustrated in Fig. 7. The slope of $\ln \Gamma(v)$ directly yields $\partial E_a/\partial v|_{v_c}$; the value of $\ln \Gamma$ at v_c gives a combination of $\ln \omega_0$ and $E_a(v_c)$, which is still not easy to cleanly disentangle [36].

However, the experiment itself offers help[4] as I now describe.

3. Vortex nucleation: thermal vs quantum

Below 0.15 K, v_c ceases abruptly to vary with T, as seen in Fig. 5. For ultra-pure ^{4}He (less than 1 part in 10^9 of ^{3}He impurities), $v_c(T)$ remains flat down to the lowest temperatures ($\sim$12 mK) reached in the experiment. The crossover from one regime to the other is very sharp. At the same crossover temperature T_q, Δv_c also levels off sharply. It is believed on experimental grounds that this saturation is intrinsic and is not due to stray heating or parasitic mechanical vibrations; this question is of paramount importance and considerable efforts have been devoted to lift all uncertainties and completely elucidate the matter [7].

Even if all possibilities of an experimental artifact are cleared out, the mere observation of a plateau in v_c is no sufficient proof for a crossover from the thermal regime to the quantum one: the effect of ^{3}He impurities, shown in the insert of Fig. 5, also gives a levelling-off of v_c vs T. This effect has been studied in detail in Ref. [33] and is well understood. Incidentally, it shows that the phase slip phenomenon taking place in the micro-aperture tracks the temperature down to below $\sim$12 mK, the lowest temperature in these experiments: there is no spurious temperature saturation effect.

If the nucleation barrier were undergoing an abrupt change at T_q, for instance because of a bifurcation toward a vortex instability of a different nature [24], in all likelihood Δv_c would jump to a different value characteristic of

4 "Nature is trying to tell us something", an idiom often used by Douglas Osheroff in connection with helium physics.

the new process (presumably small since v_c reaches a plateau). Such a jump is not observed in Fig. 6. Furthermore, v_c levels off below T_q, which would imply through Eq. (7) that E_a becomes a very steep function of v, but Δv_c also levels off, which, through Eq. (8), would imply the contrary. This remark leads us to investigate the possibility that, below T_q, thermally-assisted escape over the barrier gives way to quantum tunnelling under the barrier [37]. This transition would induce plateaus below T_q for both v_c and Δv_c.

I state again that, during the course of these investigations at Orsay-Saclay, the group of Peter McClintock at Lancaster concluded in their ion propagation studies, that there existed a crossover around 300 mK from a thermal to a quantum regime for the nucleation of vortices [38], as predicted by Muirhead, Vinen, and Donnelly [4]. There certainly are significant differences between the ion limiting drift velocity and aperture critical flow—in particular, the latter is nearly one order of magnitude smaller—but the qualitative similarities are striking. We thus have two completely different types of experiments that point toward vortex nucleation, both in a thermal regime and in a quantum one.

3.1. The macroscopic quantum tunnelling rate

To proceed with our investigation, let us now make the assumption that below T_q, zero point fluctuations do take over thermal fluctuations. The potential barrier is not surmounted with the assistance of a large thermal fluctuation, it is tunnelled under quantum-mechanically; non-conservation of energy is not a problem if it is brief enough, as stated by the Heisenberg uncertainty principle for energy. The quantum-tunnelling event is "assisted" by the zero point fluctuations [39]. What is remarkable here, and not necessarily easy to admit, is that such an energy non-conserving process does affect a macroscopic number of atoms, that are necessary to form a vortex of about 50 Å in length, as we shall see below.

Such "macroscopic quantum tunnelling" (MQT) processes have been the object of numerous experimental and theoretical studies, mainly in superconducting Josephson devices. The case of vortices in helium can be treated in a very similar manner, as done in Ref. [9]. Before giving a brief relation of MQT for vortices in ^{4}He, I summarise some of the basic results of the extended body of theoretical studies that followed Caldeira and Leggett's original work [40].

The quantum tunnelling rate of escape out of a potential well $V(q)$ is a textbook problem [41]. The rate is proportional to $\exp(-S/\hbar)$, S being, in the WKB approximation, the action of the escaping particle along the saddle-point trajectory at the top of the potential barrier, the so-called "bounce" [42]. For a particle of mass m and energy E escaping from a one-dimensional barrier $V(q)$, this action reads

$$S = 2\int_{q_1}^{q_2} \mathrm{d}q\,\sqrt{2m\big[V(q) - E\big]} \tag{9}$$

The determination of the bounce yields the points q_1 and q_2 at which the particle enters and leaves the barrier.

A discussion of the quantum tunnelling of vortices thus requires a Lagrangian formulation of vortex dynamics. Such a formulation has been carried out in particular by Sonin [14] (see also Ref. [43] for an extended discussion). However, analytical results can be obtained only at the cost of approximations and yield less than fair comparison with experiments (see the discussion in Ref. [8]).

Here, I follow, as in Ref. [9], the usual approach taken in the literature for Josephson devices [40,44], which is to choose for $V(q)$ a simple analytic form limited to a parabolic and cubic term in q:

$$V(q) = V_0 + \frac{1}{2}m\omega_0^2 q^2\left(1 - \frac{2q}{3q_b}\right) \tag{10}$$

where ω_0 is the angular frequency of the lowest mode of the trapped particle and q_b the generalised coordinate of the barrier top location. The barrier height E_b is equal to $m\omega_0^2 q_b^2/6$.

This simple form is of general applicability when the applied velocity is close to the limit, which I call v_{c0}, where the energy barrier vanishes and the system "runs away", the so-called "lability" point. At this point, the critical velocity is reached even in the absence of thermal or quantum fluctuations. Such a hydrodynamic instability threshold at which vortices appear spontaneously has been shown to occur in numerical simulations of flows past an obstacle using the Gross–Pitaevskii equation by Frisch et al. [45] and others [46–48].

The zero-temperature WKB tunnelling rate for the cubic-plus-parabolic potential E_b, Eq. (10), is found to be [40]

$$\Gamma_0 = \frac{\omega_0}{2\pi}\left(120\pi\frac{S_0}{\hbar}\right)^{1/2}\exp\left(-\frac{S_0}{\hbar}\right) \tag{11}$$

the action S_0 being equal to $36E_b/5\omega_0$.

From this result, we may anticipate that the crossover between the quantum and the thermal regime lies around a temperature close to that for which the exponents in Eqs. (5) and (11) are equal, namely $T = 5\omega_0/36k_B$—assuming that the activation energy in Eq. (5), E_a, reduces to the simple cubic-plus-parabolic form, E_b. A more precise study of the mathematical properties of the quantum channel for escape leads to the following relation [49][5]

$$\hbar\omega_0 = 2\pi k_B T_q \tag{12}$$

Once the crossover temperature has been determined from experiment, ω_0 is fixed to pinpoint accuracy compared to the fitting procedure outlined in the previous section. This is where we get help from the experiment because both the value of ω_0 is now completely pinned down and the interpretation of the experiment in terms of a nucleation process is confirmed. The values of the barrier height E_b at each given velocity then follow easily, using the full expressions for the rate in terms in terms of E_b, ω_0 and, also, the damping parameter α.

3.2. Friction in MQT

Damping turns out to matter significantly in the quantum tunnelling of semi-macroscopic objects. The relevance and applicability of the concept of quantum tunnelling to macroscopic quantities such as the electric current through a Josephson junction or the flow of superfluid through a micro-aperture, although still sometimes questioned, have been checked in detail for the Josephson effect case [50]. One of the conceptual difficulties, besides the large number of particles involved, is that the macroscopic system is coupled to an environment that acts as a thermal bath; this coupling gives rise to a source of fluctuations and semi-classical friction. This issue was tackled by Caldeira and Leggett [40], and a number of other authors (see, for instance, [49]). In the case of weak ohmic damping ($\alpha \ll 1$) and for the cubic-plus-parabolic potential, the tunnelling rate takes the form [40,51,52]:

$$\Gamma_{qt} = \frac{\omega_0}{2\pi}\left(864\pi\frac{E_b}{\hbar\omega_0}\right)^{1/2}\exp\left\{-\frac{36}{5}\frac{E_b}{\hbar\omega_0}\left[1+\frac{45\zeta(3)}{\pi^3}\alpha\right]+\frac{18}{\pi}\alpha\frac{T^2}{T_q^2}+\mathcal{O}\left(\alpha^2,\alpha\frac{T^4}{T_q^4}\right)\right\} \tag{13}$$

Thus, according to Eq. (13), damping depresses the MQT escape rate at $T = 0$—α is a positive quantity—and introduces a temperature dependence that increases the rate as T increases. These effects are large, even for weak damping, because they enter the exponent of the exponential factor in Eq. (13). Relation (12) between T_q and ω_0 is nearly unaffected by damping: ω_0 is simply changed into $\omega_0[(1+\alpha^2)^{1/2} - \alpha]$ according to Eq. (5), a minor modification for $\alpha \ll 1$.

Eq. (13) is valid up to about $T_q/2$. From $T_q/2$ to $\sim T_q$, one has to resort to numerical calculations [51]. In the thermal activation regime, $T \gtrsim T_q$, quantum corrections affect the Kramers escape rate up to about $3T_q$ and can be evaluated analytically. These high-temperature quantum corrections depend only weakly on friction. A complete solution of the problem of the influence of friction, weak, moderate or strong, in the regime where thermal fluctuations still prevail but quantum corrections cannot be neglected has first been worked out in the classical regime ($T \gg T_q$) by Grabert [53]. The extension to the temperature range $T \gtrsim T_q$ was then carried out by Rips and Pollak [54] who showed that the rate for arbitrary damping in the temperature range $T > T_q$ can be factorised into physically meaningful terms:

$$\Gamma = f_q \Upsilon \Gamma_K \tag{14}$$

namely, the classical Kramers rate Γ_K, the quantum correction factor f_q, and the depopulation factor Υ. The high temperature limit of f_q is

$$f_q = \exp\left\{\frac{\hbar^2}{24}\frac{(\omega_0^2+\omega_b^2)}{(k_B T)^2} + \mathcal{O}\left(\alpha/T^3, 1/T^4\right)\right\} \tag{15}$$

in which ω_0 and ω_b are the confining potential parameters depicted in Fig. 8. Analytic results for f_q are known to slightly below T_q [51,55].

[5] See Ref. [9] for further justifications and references to the literature.

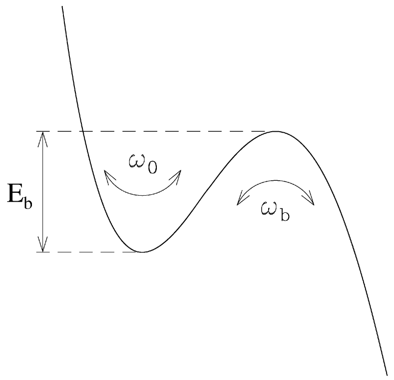

Fig. 8. Potential well trapping a particle in one dimension. The particle can escape to the continuum of states to the right. The lowest mode at the bottom of the well has angular frequency ω_0; ω_b would be the corresponding quantity if the potential was inverted bottom over top. There can exist intermediate energy levels within the well, which are populated according to the Boltzmann factor.

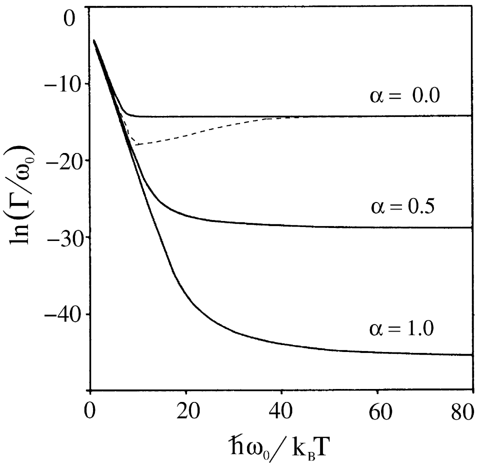

Fig. 9. Logarithm of the escape rate normalised to the attempt frequency in terms of inverse temperature, also normalised to ω_0 for various value of the damping parameter, adapted from Ref. [51]. The dot–dot line is a hand-sketch of the situation where α increases with temperature, starting from zero at $T = 0$.

The depopulation factor Υ describes the fact that the escape process eventually depletes the occupancy of the energy levels inside the potential well. This factor, the expression of which is too bulky to be reproduced here (see Ref. [54]), is unity at large α when the coupling of the Brownian particle with the thermal bath is large. It decreases to zero as $\alpha \to 0$ and the system becomes effectively decoupled from the environment. In the quantum regime, dominated by zero point fluctuations, level depletion does not take place and Υ is unity. For the nucleation of vortices, friction turns out to always be both sufficient and not too large so that depopulation corrections remain small and $\Upsilon \sim 1$.

The escape rate calculated for three values of the damping parameter α over the full temperature range is shown in Fig. 9. A hand sketch shows the influence of a temperature dependence in the damping coefficient. Such a situation is found in the nucleation of vortices in ^{4}He as I now describe.

3.3. Experimental energy barrier and damping coefficient

From this knowledge of the theoretical analytical and numerical expressions for the rate Γ, obtained for the cubic-plus-parabolic potential, it becomes possible to extract from the measured nucleation rate and crossover temperature the values of the energy barrier in terms of v_c. The value of ω_0 given by Eq. (12) ($\omega_0/2\pi = 2 \times 10^{10}$ Hz for $T_q = 0.147$ K) is consistent with the attempt frequency appropriate to the thermally-activated regime [36] and that found directly from the fits to the probability p as shown in Fig. 7. Furthermore, it agrees well (for $a_0 = 4.5$ Å) with the eigenfrequency of the highest Kelvin mode that a vortex filament in ^{4}He can sustain, $\omega_+ = \kappa_4/\pi a_0^2 = \omega_0$. The final step consists to extract the values for the energy barrier E_b from the measured escape rate. These values of E_b in the case of the experiments on ultra-pure ^{4}He analysed in Ref. [9] are shown in Fig. 10.

The self-consistency of the procedure can be checked by using the values of ω_0 and E_b derived from this analysis of the nucleation rate to compute v_c and Δv_c using Eqs. (7) and (8), mutatis mutandis, and compare with the experimentally determined values. We thus have a form of closure procedure to check the analysis, from which we conclude that our assumption according to which vortices are nucleated by quantum tunnelling below T_q shows full consistency with the thermally-assisted nucleation regime that prevails above T_q.

The quantitative analysis can be carried out one step further by constructing a Arrhenius plot from the experimental data and comparing directly the outcome to the results from theory. Arrhenius plots are drawn at constant E_b and varying temperature. Our results here are obtained at velocities that vary with temperature, hence at varying E_b's.

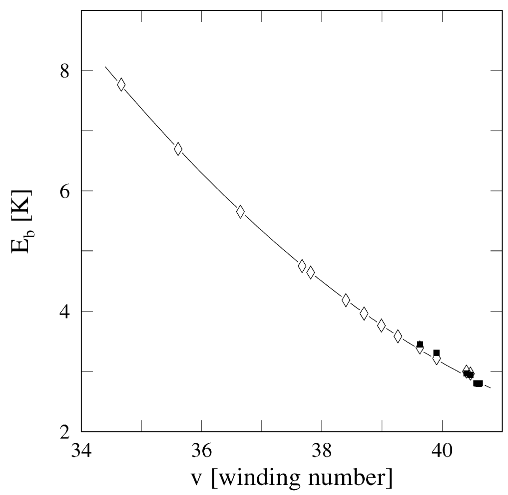

Fig. 10. The barrier energy E_b in kelvin vs v, the velocity in the aperture expressed in phase winding number obtained: (■), from the LT data transformed using the numerical tables in Ref. [51]; (◇), from the high temperature data. The high T and low T analyses yield consistent results in the region where they overlap.

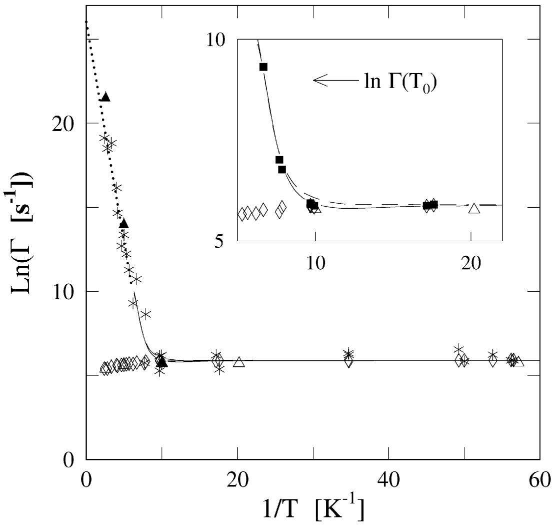

Fig. 11. $\ln\Gamma(v)$ vs $1/T$, Γ being expressed in s^{-1} and T in K: (◇), as measured at varying T and v_c; (∗), corrected for the change of the velocity with T as explained in the text. The raw data from the run with the second sample of ultra-pure ^{4}He, (△), (▲), agree very well with that of the first sample. In the inset, $\ln\Gamma(v_\mathrm{q})$, (■), has been obtained with smoothed values of v_c. The curves represent the calculated values of $\ln\Gamma(v_\mathrm{q})$ with $\alpha = 0$ (dash–dash) or varying with T (plain) as explained in the text. The dot–dot curve is the extrapolation to $1/T = 0$ of a linear fit to the high temperature portion of the data.

As can be noted in Fig. 11, the raw experimental, velocity-dependent, rates exhibit little variation over the range of parameters: escape rates are only observed in a certain window determined by experimental techniques. At low temperatures, $T < T_\mathrm{q}$, the critical velocity is close to its zero temperature limit v_q and the corrections to Γ are small. As T increases above T_q, v_c decreases and Γ has to be determined by piecewise integration of $\mathrm{d}\ln\Gamma/\mathrm{d}v$. The high temperature extrapolation for Γ obtained in such a manner does display the expected $1/T$ dependence, as seen in Fig. 11.

The low temperature corrected Γ shows, as can be seen in the inset of Fig. 11, a small, but real, drop below its zero temperature limit as the temperature is raised, thereby simply following the trend of the measured Γ. As illustrated in Fig. 9, this drop reveals the influence of damping. A damping coefficient α that increases from 0 at $T = 0$ to ~ 0.1 around T_q and more slowly above accounts for the observed drop [9]. This T-dependent dissipation also makes the crossover between the thermal and the quantum regimes even sharper than for $\alpha = 0$, and closer to observations. The nucleation of vortices in ^{4}He thus offers a rare observation of the effect of damping on MQT.

4. The vortex half-ring model

As described in the previous section, there is strong evidence that the experimental features of the phase slip data result from quantised vortex nucleation. The nucleation barrier E_b is of the order of a few kelvins (see Fig. 10). The attempt frequency $\sim 2 \times 10^{10}$ Hz is of the order of the highest Kelvin waves mode. In this section, I wish to describe a simple model that will account for the features described above. This model, the nucleation of vortex half-rings at a prominent asperity on the walls, finds its roots in the work of Langer, Fischer, and Reppy [3,56], Volovik [57], and Muirhead, Vinen and Donnelly [4]. It was further developed and put on firm experimental findings in Ref. [7].

The model premise is quite simple. Consider, as done by Langer and Reppy in Ref. [3], the homogeneous nucleation of a vortex ring in a homogeneous flow v_s. When the ring has reached radius R in a plane perpendicular to the flow, its

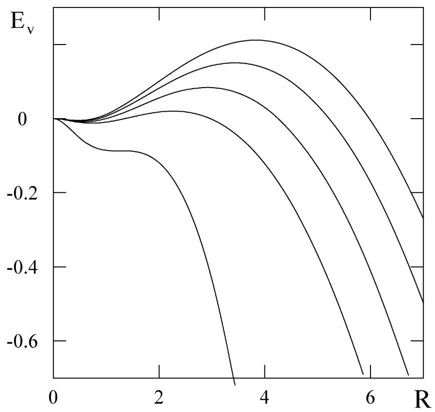

Fig. 12. Energy barrier E_{v} vs R, the vortex radius, in the simple half-ring model at various superfluid flow velocities. This figure is taken from Ref. [7] and applies for the model and with the units used in that reference. It is given here for illustration purposes, namely that potentials of the form of Eq. (16) give rise to confining wells.

energy in the laboratory frame, where the observer is at rest and sees the superfluid moving at velocity v_{s}, is expressed by

$$E_{\mathrm{v}} = E_R - P_R v_{\mathrm{s}} \tag{16}$$

The rest energy E_R and impulse P_R of the vortex ring are given by Eqs. (2) and (3). The minus sign in the right-hand side of Eq. (16) arises because I have implicitly assumed that the vortex opposes the flow, i.e., that its impulse P_R points straight against v_{s}: this configuration minimises E_{v}.

The rest energy E_R increases with vortex size as $R \ln R$ and the impulse P_R as R^2: the impulse term becomes dominant at large radii and causes E_{v} to become negative. The variation of E_{v} in terms of R has the shape of a confining well potential, which becomes shallower and shallower with increasing v_{s}, as depicted in Fig. 12. The barrier height can easily be computed numerically and substituted into the expression for v_{c}, Eq. (7). An analytical approximation for v_{c} involving the neglect of logarithmic terms and valid for large vortices ($R \gg a_0$) has been given by Langer and Reppy [3].

Such a critical velocity would be for the formation of a mist of vortices in the bulk of the superfluid. However, this sort of vorticity condensation does not take place for two reasons. Firstly, the velocity of potential flows, which follows from the Laplace equation, reaches its maximum value at the boundaries, not in the bulk. Secondly, the nucleation of a vortex half-ring at the boundary itself involves a half of the energy given by Eq. (16). Hence, half-ring nucleation at the wall is always much more probable at the same velocity v_{s} than full ring nucleation in the bulk. Half of the energy for the half-ring holds for classical hydrodynamics, the other half being taken care of by the image in the plane boundary. For a superfluid vortex, the actual energy of a half-ring is smaller than in the classical ideal fluid because the superfluid density is depleted at the solid wall and the core radius increases. This effect strengthens the case for half-rings, as discussed in Ref. [23].

The barrier height can easily be computed and substituted into the expressions for v_{c} and Δv_{c}, Eqs. (7) and (8). Critical velocities v_{c} and statistical widths Δv_{c} computed in such a manner are shown as a function of temperature in Figs. 5 and 6 for several values of the vortex core parameter a_0. A value of 4.5 Å gives near-quantitative agreement with the experimental observations over the entire temperature range. This value of a_0 is compatible not only with the temperature variations of v_{c} and Δv_{c} but also with the magnitude of the *local* v_{c} found to be 20–22 m/s using ^{3}He impurities as a local velocity probe [33]. It exceeds that in the bulk ($a_0 \simeq 2.5$ Å), which is thought to reflect the proximity of the wall as discussed in greater details in Ref. [8]. With this value, the nucleating half-ring has a radius of approximately 15 Å at the top of the barrier.

Once nucleated, the vortex floats away, carried out by the superfluid stream at the local superfluid velocity and by its own velocity, $v_R = \partial E_R / \partial P_R$. It can be noted that, at the top of the barrier, $\partial E_{\mathrm{v}} / \partial R = 0$ and the vortex self-velocity v_{R} exactly balances the applied v_{s}: the nucleating vortex is at a near standstill.

If the flow is uniform, with parallel streamlines, nothing much happens; the vortex wanders away and the interaction with the normal fluid and with the wall causes a loss of vortex energy that eventually leads to its disappearance. If the

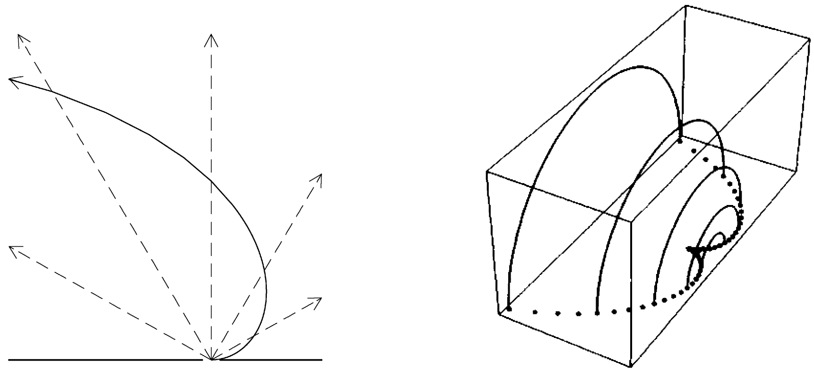

Fig. 13. 2D (left) and 3D (right) views of the vortex half-ring trajectory over a point-like orifice in an infinite plane. The dash–dash lines on the 2D plot are the potential flow lines that emerge from the orifice.

flow is divergent, as in Fig. 13, the vortex tends to follow the local streamlines and grows under the combined action of the potential flow and its own self-velocity: it then gains energy at the expense of the potential flow. In such a way, it can expand from nanometric to micrometric sizes and above. The vortex in its motion away from the micro-aperture takes a finite lump of energy to remote places of the cell. This energy loss reduces the Helmholtz resonance amplitude in a fairly sudden manner. Such a dissipative event gives the signature of single phase slips that is seen in Fig. 3.

This scenario for a phase slip involves a change of the phase difference between the two sides of the micro-aperture of exactly 2π because the vortex ends up crossing all the streamlines, as pictured in Fig. 13. This crossing causes the velocity circulation to change by exactly one quantum κ_4 on all the superfluid paths extending from one side of the aperture to the other.

5. Pinning, vortex mills, collapses and all that

Single phase slips are observed in experimental situations which may be loosely characterised as "clean", that is, for uncontaminated apertures of relatively small sizes (a few micrometres at the most), with low background of mechanical and acoustical interferences, etc., and with probing techniques that do not manhandle the superfluid, namely, with low frequency Helmholtz resonators. When these conditions are not met, flow dissipation occurs in a more or less erratic manner in large bursts—multiple phase slips or 'collapses' of the superflow.

Multiple phase slips and collapses constitute an apparent disruption of the vortex nucleation mechanism described in the previous section. Their properties have been studied in detail in Ref. [22] and are briefly mentioned below, together with possible mechanisms for their formation. It is likely that these events provide a bridge between the "clean" single phase slip case and the usual situation of the Feynman type critical velocities that are temperature-independent below 1 K and dependent on the channel size. This problem, which is not fully resolved at present, almost certainly involves some form of pre-existing vorticity.

5.1. Remnant vorticity and vortex mills

Remnant vorticity in ^{4}He, which has long been assumed, has been shown directly to exist by Awschalom and Schwarz by looking at the trapping of ions by vortex lines [58]. Vortices, presumably nucleated at the λ transition where the critical velocity is very low, remain stuck in various places of the superfluid sample container. This trapped vorticity, according to Adams et al. [59], either is quite loosely bound to the substrate and disappears rapidly, or is strongly pinned and is dislodged only by strong perturbations.

To account for laboratory observations and with the outcomes of numerous numerical simulations of vortex dynamics, Schwarz has proposed the following formula for the velocity at which vortices unpin [60],

$$v_{\mathrm{u}} \lesssim \frac{\kappa_4}{2\pi D} \ln\left(\frac{b}{a_0}\right) \tag{17}$$

D being the size of the pinned vortex and b being a characteristic size of the pinning asperity. Eq. (17) bears a strong resemblance with that for the Feynman critical velocity, Eq. (4). Long vortices unpin at very low velocities unless they are perched on a tall pedestal, but very small vortices pinned on microscopic defects at the cell walls can in principle exist under a wide range of superflow velocities; a 200 nm long vortex filament pinned at both ends on 20 Å asperities resists transverse flows of velocities up to 10 cm/s.

In connection with the critical velocity problem, the long standing suggestion by Glaberson and Donnelly [61] of vortex mills still prevails. In these authors' views, imposing a flow on a vortex pinned between the opposite lips of an aperture would induce deformations such that the vortex would twist on itself, undergo self-reconnections, and mill out free vortex loops. First, we note that, according to Eq. (17), such a mill must involve a pinned vortex of sub-micrometric size for any flow velocity above $\sim$1 cm/s in order for the pinned vortex not to be washed away. Thus, it cannot as such account for Feynman-type critical velocities found in large channels. Also, as shown by numerical simulations of 3D flows involving few vortices only [62], vortex loops and filaments are stable even against large deformations. Vortices are not prone to twist on themselves and foster loops. It takes the complex flow fields associated with fully developed vortex tangles to produce small rings [63,64]. And it takes some quite special vortex pinning geometry to set up a mill that actually works.

Schwarz has demonstrated the existence of such a mill by numerical simulations [65]. Let us take a vortex pinned at one end and floating along the flow streamlines with its other end moving freely on the wall; this vortex develops a helical motion, a sort of driven Kelvin wave, and reconnects sporadically to the wall when the amplitude of the helical motion grows large enough. This helical mill, which has to be of sub-micrometric size to stand the flow, does churn out fresh vortices.

Vortex mills are thus unlikely to explain the critical velocities of the Feynman type in the simple scheme suggested by Glaberson and Donnelly [61]. However, the occurrence of multiple slips, which can be seen in Fig. 3, is probably caused by some form of vortex mills on a microscopic size. Before coming to this topic, I need to describe multiple slips in greater details. But, at this point, the above remarks on the stability of vortex loops or half-loops in their course already make it unlikely that multiple slips be due to the production of small rings by the nucleating vortices twisting on themselves à la Glaberson–Donnelly, as suggested by Amar et al. [66]. We have to dig a little further to devise a scheme that works.

5.2. *The two types of large slips*

Besides the usual single slip pattern, there appears in Fig. 3 occasional double slips (i.e. involving phase changes by 4π) and infrequent triple slips. Raising the temperature to 80 mK, again for this particular cool-down, causes these multiple slips to occur much more frequently and to involve more circulation quanta on the mean. These features are described in detail in Ref. [22]. As the probability for a one-slip event per half-cycle is not large, that for a double slip is small, and it becomes negligible for higher multiples. A separate mechanism for their formation must be found.

Some degree of understanding of the formation of multiple slips can be gained by plotting the mean value of the phase slip sizes, expressed in number of quanta, against the flow velocity at which the slips take place [67]. This flow velocity is close to the critical velocity for single phase slips, i.e. the vortex nucleation velocity; it varies with temperature, pressure, and resonator drive level. A plot summarising these variations is shown in Fig. 14 for $\langle n_+\rangle$, i.e. in the flow direction conventionally chosen as the $+$ direction. Slips in the opposite $(-)$ direction behave qualitatively in the same manner but the phenomenon displays a clear quantitative asymmetry. As can be seen in Fig. 14, the mean slip size decreases, as does the nucleation velocity, on either side of the quantum plateau—a ^{3}He impurity effect on the low T side—a thermal effect on the high-T side. However, it increases with pressure, contrarily to the nucleation velocity which decreases with increasing pressure.

We conclude from the organisation of the data with the various parameters in Fig. 14 that the magnitude of the superflow velocity does not directly control, by itself, the occurrence of multiple slips. In turn, this implies, as will be discussed further below, that the phenomenon under study is not purely ruled by hydrodynamics in the bulk of the fluid but involves some complex interplay with the boundaries. As shown in Fig. 14, the velocity threshold for the appearance of multiple slips depends on hydrostatic pressure; in fact, the P-dependence of the upturn of $\langle n_+\rangle$ vs v exactly tracks that of the critical velocity for single phase slip nucleation. This indicates that multiple slips appear because of an alteration, or as a consequence, of the nucleation process itself.

The pattern of formation of multiple slips changes from cool-down of the cell from room temperature to cool-down but remains stable for each given cool-down. It seems to depend on the degree of contamination of the cell, a degree

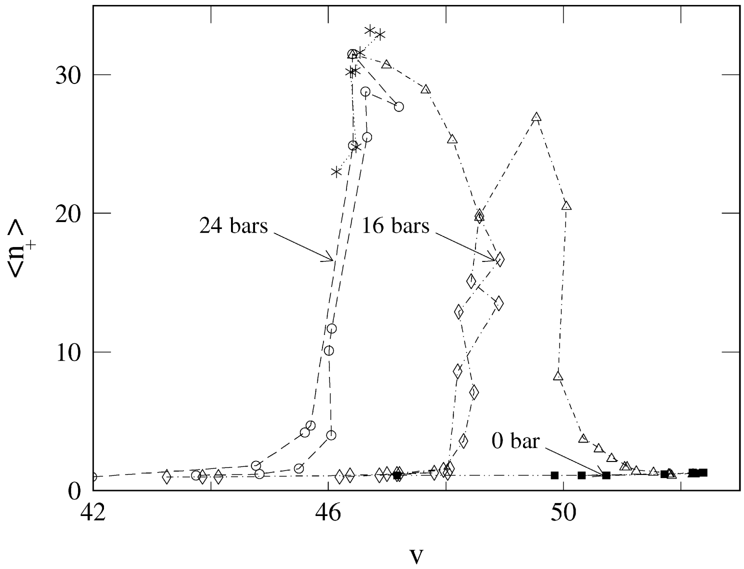

Fig. 14. Mean size of (positive) multiple slips vs velocity in phase winding number in nominal purity ^{4}He (100 ppb ^{3}He): (△) pressure sweep from 0.4 to 24 bars at 81.5 mK (all even values of the pressure P, and 0.4, 1, 3, 5, 7 bars)—(⋄) temperature sweep at 16 bars—(∘) temperature sweep at 24 bars—(∗) drive level sweep at 24 bars, 81.5 mK—(■) temperature sweep at 0 bar. For the temperature sweeps, from 14 to 200 mK approximately, v first increases, reaches the quantum plateau and then decreases, as shown in the insert of Fig. 5. Lines connect successive data points in the temperature and pressure sweeps.

which cannot easily be controlled experimentally. The detailed microscopic configuration of the aperture wall where nucleation takes place probably plays an major rôle in multiple slip formation.

Another kind of very large drops in the resonance amplitude of the resonator was also observed, which sometimes resulted in a complete collapse of the resonance. These "singular" collapses, first observed by Hess [68], occur at flow velocities that are lower than the critical velocity for phase slips, sometimes as low as $v_c/3$. Multiple slips are different from "singular" collapses and the underlying mechanisms responsible for both phenomena are bound to be different, as discussed below.

5.3. In-situ contamination by atomic clusters: pinning and collapses

In a series of experiments conducted at Saclay [69,70], in which the experimental cell was deliberately heavily contaminated by atomic clusters of air or H_2, we observed that numerous multiple slips and collapses of the "singular" type occurred. The peak amplitude charts of the resonator became mostly impossible to interpret, except in a few instances where two apparent critical velocities for single phase slips were observed. The higher critical velocity corresponds to the one observed in the absence of contamination. The lower critical velocity is thought to reveal the influence of a vortex pinned in the immediate vicinity of the nucleation site. This vortex induces a local velocity which adds to that of the applied flow and causes an apparent decrease in the critical velocity for phase slips. Because of this change, the presence of the pinned vortex could be monitored, the lifetime in the pinned state and the unpinning velocity could be measured, yielding precious information on the pinning process.

This observation, reported in detail in Refs. [69] and [70], shows that pinned vorticity can contribute to the nucleation of new vortices at the walls of the experimental cell. Such pinned vortices as the one described above can, instead of interacting with the nucleation site, set up a transient vortex mill of the helical type and generate a burst of vortices. The existence of such pinned vortices is established; that they can form a micro-mill is highly plausible. We thus have a possible explanation for multiple slip formation [8]. The pinning event would take place immediately after nucleation when the velocity of the vortex relative to the boundary is still very small and the capture by a pinning site easy. The micro-mill remains in activity as long as the flow is sufficient to maintain the helical instability, which depends on the pinning stand geometry. As it is set up to withstand one flow direction, it is destroyed when the flow velocity reverses itself in the resonance motion. It eventually re-establishes itself during a subsequent resonance cycle, causing a new multiple slip. This process depends on the precise details of the pinning site configuration and of the primordial vortex trajectory, factors which allow for the variableness of multiple slips on contamination and pressure.

In the same experiments, we also observed that a large number of unpinning events were taking place at an "anomalously low" unpinning velocity. A parallel can be made [70] with the singular collapses that also occur at "subcritical" velocities. In fact, both phenomena were seen quite frequently in these experiments, suggesting that they have a common cause. Noting furthermore that pinning and unpinning processes were also quite frequent, releasing a fair amount of vagrant vorticity, it appears quite plausible that both singular collapses and low velocity unpinning events are caused by vagrant vortices hopping from pinning sites to pinning sites, eventually passing by close to a pinned vortex or a vortex nucleation site, and giving a transient boost to the local velocity, which pushes a pinned vortex off its perch or causes a burst of vortices to be shed.

These observations, albeit incidental, have important consequences for the critical velocity problem: existing vortices, either pinned or free-moving, can contribute to the nucleation of new vortices at the walls of the experimental cell at apparent velocities much lower than the critical velocity for phase slips. We are thus provided with a mechanism by which superflow dissipation sets in at mean velocities on the large scale much smaller the velocity for vortex nucleation on the microscopic scale, possibly bridging the gap between phase slip and Feynman type critical velocities. Vortex nucleation at the walls is also quite likely to take part in the build-up of self-sustaining vortex tangles forming superfluid turbulence, up to now attributed solely to reconnection mechanisms [71].

To conclude, the critical velocities in superfluids that are true and proven include the Landau critical velocity for roton creation, the formation of vortices by a hydrodynamical instability in BEC gases [72] and in ^{3}He [73], the nucleation of vortices by thermal activation and quantum tunnelling in ^{4}He, both for ion propagation and in aperture flow. I have presented rather compelling experimental evidence for the interplay between vortex nucleation and pinned vorticity on a microscopic scale; this evidence points toward the existence of helical vortex micro-mills that can generate vortices at fairly low applied velocities. Finally, vagrant vortices interacting with these mills, or with vortex nucleation sites, are found to generate enough vorticity to completely kill the applied superflow and explain singular collapses. The study of phase slippage has taken us a long way toward an explanation of critical velocities in superfluid helium-4.

References

[1] J. Wilks, The Properties of Liquid and Solid Helium, Clarendon Press, Oxford, 1967.
[2] W. Vinen, Critical velocities in liquid helium II, in: G. Careri (Ed.), Liquid Helium, Academic Press, New York, 1963, p. 336.
[3] J. Langer, J. Reppy, in: C.J. Gorter (Ed.), Prog. Low Temp. Phys., vol. 6, North-Holland, Amsterdam, 1970, p. 1, Chapter 1.
[4] C. Muirhead, W. Vinen, R. Donnelly, The nucleation of vorticity by ions in superfluid ^{4}He i. Basic theory, Phil. Trans. Roy. Soc. A 311 (1984) 433.
[5] E. Varoquaux, O. Avenel, M. Meisel, Phase slippage and vortex nucleation in the critical flow of superfluid ^{4}He through an orifice, Can. J. Phys. 65 (1987) 1377.
[6] E. Varoquaux, W. Zimmermann Jr., in: A.F.G. Wyatt, H.J. Lauter (Eds.), Excitations in Two-Dimensional and Three-Dimensional Quantum Fluids, Plenum Press, New York, 1991, p. 343.
[7] O. Avenel, G. Ihas, E. Varoquaux, The nucleation of vortices in superfluid ^{4}He: Answers and questions, J. Low Temp. Phys. 93 (1993) 1031.
[8] E. Varoquaux, O. Avenel, Y. Mukharsky, P. Hakonen, The experimental evidence for vortex nucleation in ^{4}He, in: W.F. Vinen, C.F. Barenghi, R.J. Donnelly (Eds.), Quantized Vortex Dynamics and Superfluid Turbulence, Springer-Verlag, Berlin, 2001, p. 36.
[9] E. Varoquaux, O. Avenel, Vortex nucleation in phase-slippage experiments in ultrapure superfluid ^{4}He below 0.5 K, Phys. Rev. B 68 (2003) 054515.
[10] G. Baym, in: R.C. Clark, G.H. Derrick (Eds.), Mathematical Methods in Solid State and Superfluid Theory, Oliver and Boyd Ltd, Edinburgh, 1969, p. 134, Chapter 3.
[11] P. Anderson, Considerations on the flow of superfluid helium, Rev. Mod. Phys. 38 (1966) 298.
[12] S.H. Lamb, Hydrodynamics, sixth ed., Cambridge Univ. Press, Cambridge, UK, 1932.
[13] E. Sonin, Vortex oscillations and hydrodynamics of rotating superfluids, Rev. Mod. Phys. 59 (1987) 87.
[14] E. Sonin, Nucleation and creep of vortices in superfluids and clean superconductors, Physica B 210 (1995) 234.
[15] O. Avenel, E. Varoquaux, Observation of singly quantized dissipation events obeying the Josephson frequency relation in the critical flow of superfluid ^{4}He through an aperture, Phys. Rev. Lett. 55 (1985) 2704.
[16] G. Shifflett, G. Hess, Intrinsic critical velocities in superfluid ^{4}He flow through 12-μm diam. orifices near T_λ: Experiments on the effect of geometry, J. Low Temp. Phys. 98 (1995) 591.
[17] W. Zimmermann Jr., The flow of superfluid ^{4}He through submicron apertures: phase slip and critical velocities due to quantum vortex motion, Contemp. Phys. 37 (1996) 219.
[18] R. Packard, The role of the Josephson–Anderson equation in superfluid helium, Rev. Mod. Phys. 70 (1998) 641.
[19] O. Avenel, E. Varoquaux, Josephson effect and phase slippage in superfluids, Jpn. J. Appl. Phys. 26 (1987) 1798.

[20] B.P. Beecken, W. Zimmermann Jr., Variation of the critical order-parameter phase difference with temperature from 0.4 to 1.9 K in the flow of superfluid ^{4}He through a tiny orifice, Phys. Rev. 35 (1987) 1630.
[21] E. Varoquaux, O. Avenel, Phase slip phenomena in superfluid helium, Physica B 197 (1994) 306.
[22] O. Avenel, M. Bernard, S. Burkhart, E. Varoquaux, Autopsy of superflow collapses and multiple phase slips, Physica B 210 (1995) 215.
[23] S. Burkhart, M. Bernard, O. Avenel, E. Varoquaux, Scenario for a quantum phase slip, Phys. Rev. Lett. 72 (1994) 380.
[24] C. Josserand, Y. Pomeau, Generation of vortices by the Kadomtsev–Petviashvili instability, Europhys. Lett. 30 (1995) 43.
[25] C. Josserand, Y. Pomeau, S. Rica, Cavitation versus vortex nucleation in a superfluid model, Phys. Rev. Lett. 75 (1995) 3150.
[26] A. Andreev, L. Melnikovsky, Thermodynamics of superfluidity, J. Low Temp. Phys. 135 (2004) 411.
[27] J. Hulin, D. D'Humières, B. Perrin, A. Libchaber, Critical velocities for superfluid helium flow through a small hole, Phys. Rev. A 9 (1974) 885.
[28] W. Zimmermann Jr., The critical velocity behavior of superfluid ^{4}He in a micron-size aperture at two different frequencies of oscillatory flow, J. Low Temp. Phys. 91 (1993) 219.
[29] P. McClintock, R. Bowley, Vortex creation in superfluid helium-4, in: A.F.G. Wyatt, H.J. Lauter (Eds.), Excitations in Two-Dimensional and Three-Dimensional Quantum Fluids, Plenum Press, New York, 1991, p. 567.
[30] P. McClintock, R. Bowley, The Landau critical velocity, in: W. Halperin (Ed.), Prog. Low Temp. Physics, vol. XIV, Elsevier, Amsterdam, 1995, p. 1.
[31] G.W. Rayfield, F. Reif, Quantized vortex rings in superfluid helium, Phys. Rev. 136 (1964) A1194.
[32] W. Zimmermann Jr., C. Lindensmith, J. Flaten, The interpretation of phase-slip and critical-velocity data, J. Low Temp. Phys. 110 (1998) 497.
[33] E. Varoquaux, G. Ihas, O. Avenel, R. Aarts, Vortex nucleation in superfluid ^{4}He probed by ^{3}He impurities, Phys. Rev. Lett. 70 (1993) 2114.
[34] J. Steinhauer, K. Schwab, Y. Mukharsky, J. Davis, R.E. Packard, Vortex nucleation in superfluid ^{4}He, Phys. Rev. Lett. 74 (1995) 5056.
[35] W. Zimmermann Jr., O. Avenel, E. Varoquaux, Critical flow of superfluid helium-4 through a submicron aperture: width of the critical transition, Physica B 165 166 (1990) 749.
[36] E. Varoquaux, M. Meisel, O. Avenel, Onset of the critical velocity regime in superfluid ^{4}He at low temperature, Phys. Rev. Lett. 57 (1986) 2291.
[37] G. Ihas, O. Avenel, R. Aarts, R. Salmelin, E. Varoquaux, Quantum nucleation of vortices in the flow of superfluid ^{4}He through an orifice, Phys. Rev. Lett. 69 (1992) 327.
[38] P. Hendry, N. Lawson, P. McClintock, C. Williams, R. Bowley, Macroscopic quantum tunneling of vortices in He II, Phys. Rev. Lett. 60 (1988) 604.
[39] J. Martinis, H. Grabert, Thermal enhancement of macroscopic quantum tunneling: Derivation from noise theory, Phys. Rev. B 38 (1988) 2371.
[40] A. Caldeira, A. Leggett, Quantum tunnelling in a dissipative system, Ann. Phys. (N.Y.) 149 (1983) 374;
A. Caldeira, A. Leggett, Quantum tunnelling in a dissipative system, Ann. Phys. (N.Y.) 153 (1984) 445 (Erratum).
[41] L. Landau, E. Lifshitz, Quantum Mechanics, first ed., Pergamon Press, London, 1958, §50.
[42] S. Coleman, Fate of the false vacuum: Semiclassical theory, Phys. Rev. D 15 (1977) 2929.
[43] U. Fischer, Tunnelling of topological line defects in strongly coupled superfluids, Ann. Phys. (Leipzig) 9 (2000) 523.
[44] A. Larkin, K. Likharev, Y. Ovchinnikov, Secondary quantum macroscopic effects in weak superconductivity, Physica B 126 (1984) 414.
[45] T. Frisch, Y. Pomeau, S. Rica, Transition to dissipation in a model of superflow, Phys. Rev. Lett. 69 (1992) 1644.
[46] C. Nore, C. Huepe, M. Brachet, Subcritical dissipation in three-dimensional superflows, Phys. Rev. Lett. 84 (2000) 2191.
[47] N.G. Berloff, P.H. Roberts, Vortices in nonlocal condensate models of superfluid helium, in: Quantized Vortex Dynamics and Superfluid Turbulence, Springer-Verlag, Berlin, 2001, p. 268.
[48] S. Rica, Vortex Nucleation and Limit Speed for a Flow Passing Nonlinearly Around a Disk in the Nonlinear Schrödinger Equation, in: Lecture Notes in Physics, vol. 571, Springer-Verlag, Berlin, 2001, p. 258.
[49] V. Mel'nikov, The Kramers problem: Fifty years of development, Phys. Rep. 209 (1991) 1.
[50] J.M. Martinis, M.H. Devoret, J. Clarke, Experimental tests for the quantum behavior of a macroscopic degree of freedom: The phase difference across a Josephson junction, Phys. Rev. B 35 (1987) 4682.
[51] H. Grabert, P. Olschowski, U. Weiss, Quantum decay rates for dissipative systems at finite temperatures, Phys. Rev. B 36 (1987) 1931.
[52] D. Waxman, A. Leggett, Dissipative quantum tunneling at finite temperatures, Phys. Rev. B 32 (1985) 4450.
[53] H. Grabert, Escape from a metastable well: The Kramers turnover problem, Phys. Rev. Lett. 61 (1988) 1683.
[54] I. Rips, E. Pollak, Quantum Kramers model: Solution of the turnover problem, Phys. Rev. A 41 (1989) 5366.
[55] P. Hänggi, P. Talkner, M. Borkovec, Reaction rate theory: Fifty years after Kramers, Rev. Mod. Phys. 62 (1990) 251.
[56] J. Langer, M. Fisher, Intrinsic critical velocity of a superfluid, Phys. Rev. Lett. 19 (1967) 560.
[57] G. Volovik, Quantum-mechanical formation of vortices in a superfluid liquid, Sov. Phys. JETP Lett. 15 (1972) 81.
[58] D. Awschalom, K.W. Schwarz, Observation of a remanent vortex-line density in superfluid helium, Phys. Rev. Lett. 52 (1984) 49.
[59] P. Adams, M. Cieplak, W.I. Glaberson, Spin-up problem in superfluid ^{4}He, Phys. Rev. B 32 (1985) 171.
[60] K. Schwarz, Three-dimensional vortex dynamics in superfluid ^{4}He: Line–line and line–boundary interactions, Phys. Rev. B 31 (1985) 5782.
[61] W. Glaberson, R. Donnelly, Growth of pinned quantized vortex lines in helium II, Phys. Rev. 141 (1966) 208.
[62] K.W. Schwarz, private communication.
[63] B. Svistunov, Superfluid turbulence in the low-temperature limit, Phys. Rev. B 52 (1995) 3647.
[64] M. Tsubota, T. Araki, S.K. Nemirovskii, Dynamics of vortex tangle without mutual friction in superfluid ^{4}He, Phys. Rev. B 62 (2000) 11751.
[65] K. Schwarz, Phase slip and turbulence in superfluid ^{4}He: A vortex mill that works, Phys. Rev. Lett. 64 (1990) 1130.
[66] A. Amar, Y. Sasaki, R. Lozes, J. Davis, R. Packard, Quantized phase slippage in superfluid ^{4}He, Phys. Rev. Lett. 68 (1992) 2624.
[67] E. Varoquaux, O. Avenel, M. Bernard, S. Burkhart, Multiple quantum phase slips in superfluid ^{4}He, J. Low Temp. Phys. 101 (1995) 821.
[68] G. Hess, Vortex generation in modulated superfluid ^{4}He flow through a pinhole, Phys. Rev. B 15 (1977) 5204.

[69] P. Hakonen, O. Avenel, E. Varoquaux, Evidence for single-vortex pinning and unpinning events in superfluid ^{4}He, Phys. Rev. Lett. 81 (1998) 3451.
[70] E. Varoquaux, O. Avenel, P. Hakonen, Y. Mukharsky, Observation of single-vortex pinning in superfluid ^{4}He, Physica B 255 (1998) 55.
[71] K. Schwarz, Critical velocity for a self-sustaining vortex tangle in superfluid helium, Phys. Rev. Lett. 50 (1983) 364.
[72] K.W. Madison, F. Chevy, V. Bretin, J. Dalibard, Stationary states of a rotating Bose–Einstein condensate: Routes to vortex nucleation, Phys. Rev. Lett. 86 (2001) 4443.
[73] V. Eltsov, M. Krusius, G. Volovik, Vortex formation and dynamics in superfluid ^{3}He, in: W. Halperin (Ed.), Prog. Low Temp. Physics, vol. XV, Elsevier, 2005, p. 1, Chapter 1.